Chemical Engineering Journal 253 (2014) 538–543

Contents lists available at ScienceDirect

Chemical Engineering Journal

journal homepage: www.elsevier.com/locate/cej

Adenovirus inactivation by in situ photocatalytically and photoelectrocatalytically generated halogen viricides

Guiying Li [a,b], Xiaolu Liu [a,b], Haimin Zhang [b], Po-Keung Wong [c], Taicheng An [a,d,*], Wenqu Zhou [d], Bing Li [d], Huijun Zhao [b,*]

[a] State Key Laboratory of Organic Geochemistry, Guangzhou Institute of Geochemistry, Chinese Academy of Sciences, Guangzhou 510640, China
[b] Centre for Clean Environment and Energy, Gold Coast Campus, Griffith University, Queensland 4222, Australia
[c] School of Life Sciences, The Chinese University of Hong Kong, Shatin, N.T., Hong Kong Special Administrative Region, China
[d] Experiment Medical Research Centre and Key Laboratory of Reproduction and Genetics of Guangdong Higher Education Institutes of The Third Affiliated Hospital, Guangzhou Medical College, Guangzhou 510182, China

HIGHLIGHTS

- Adenovirus was inactivated by in situ PC and PEC generated halogen viricides.
- The PEC-Br shows the highest virucidal efficiency.
- The PEC-Br can completely inactivate ~1000 TCID50 RDRADS within 31.7 s.
- The superior performances is mainly due to the increased productions of AOSs.

GRAPHICAL ABSTRACT

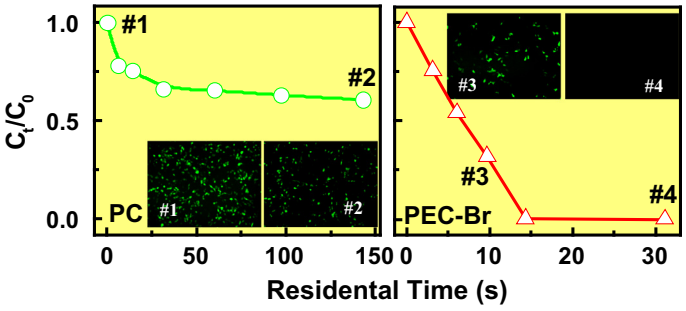

ARTICLE INFO

Article history:
Received 28 March 2014
Received in revised form 13 May 2014
Accepted 14 May 2014
Available online 22 May 2014

Keywords:
Photocatalytic inactivation
Photoelectrocatalytic inactivation
Adenovirus
Reaction mechanisms
Halides

ABSTRACT

This study investigates and compares the virucidal performances of photocatalytic (PC) and photoelectrocatalytic (PEC) treatments in the presence and absence of halides, such as Br^- and Cl^-, under comparable experimental conditions. The results confirm that the PC virucidal efficiency can be enhanced in the presence of low halide concentrations (e.g., X = Br^- or Cl^-) and further enhanced by applying potential bias onto the photoanode in a PEC system. The PEC treatment in the presence of 1.0 mM Br (PEC-Br) shows the highest virucidal efficiency, enabling complete inactivation of a ~1000 TCID50 replication-deficient recombinant adenovirus (RDRADS) population within 31.7 s. The superior virucidal performances of PEC-X treatments can be attributed to the increased production of active oxygen species and additional viricides resulting from the PEC halide oxidation, as well as prolonged lifetime of photoholes (h^+) for direct inactivation. The findings of this work confirm that new forms of active species generated in situ via a PC or PEC process are effective for viruses.

1. Introduction

The outbreak of severe acute respiratory syndrome (SARS) in February 2003, caused by the deadly coronavirus, affected 3547 individuals, resulting in 182 deaths by April 2003 [1]. In recent history, numerous emerging and re-emerging viruses have caused widespread human disease and deaths, raising worldwide fears. The most well-known examples are the avian influenza H5N1 virus

* Corresponding authors. Address: State Key Laboratory of Organic Geochemistry, Guangzhou Institute of Geochemistry, Chinese Academy of Sciences, Guangzhou 510640, China. Tel.: +86 20 85291501; fax: +86 20 85290706 (T. An). Tel.: +61 7 555 2 8261; fax: +61 7 5552 8067 (H. Zhao).
E-mail addresses: antc99@gig.ac.cn (T. An), h.zhao@griffith.edu.au (H. Zhao).

http://dx.doi.org/10.1016/j.cej.2014.05.059
1385-8947/

in 1997, the H7N9 virus in 2013, and the swine influenza H1N1 virus in 2009–2010. Although the transmission modes of viruses are diverse, wastewater is recognized as an important source of contaminated microbial aerosols and liquid. Given the importance of this factor in virus transmission [2], a number of research projects have focused on developing highly effective inactivation/separation water treatment techniques [3,4]. However, virus are submicroscopic particles. As such, the conventional filtration methods are generally less effective; furthermore, biofouling also leads to extra operational costs [5]. When considering UV and chlorination inactivation techniques, a number of pathogens, particularly some virus species, are naturally resistant to such traditional treatments [6,7]. In addition, the formations of toxic and potential carcinogenic by-products are also drawbacks of chlorine treatment [8–10]. Ozone disinfection has been considered as an effective alternative [11]; however, disadvantages, such as its toxic and corrosive characteristics, also hinder its practical application [12].

Recently developed TiO_2 photocatalysis (PC) based advanced oxidation processes for inactivation of virus have demonstrated promising outcomes [13,14]. These works have revealed the virucidal effect of PC processes at nanostructured TiO_2 on the inactivation of different viruses, including phage MS2, phage PL-1, and bacteriophage Qβ [3,15,16]. Nevertheless, PC inactivation of adenovirus has not been previously attempted, despite being indicated in the "Drinking Water Contaminant Candidate List" [17] because of their prevalent potential health risks and important role for water epidemiology [18–20]. Moreover, adenoviruses are highly resistant to common treatments when compared to other viral pathogens of concern in wastewater and drinking water [21,22], due to their DNA's double-stranded nature [23].

TiO_2 photoelectrocatalysis (PEC) has been proven to enhance the degradation efficiencies of organic pollutants in water [24], but are rarely used to improve the virus inactivation efficiency [25]. We have previously demonstrated the effectiveness of a PEC-based bactericidal technique in the presence of Br^- (PEC-Br) for instant inactivation and rapid decomposition of gram-negative bacteria [26,27]. In this study, we investigate the application of PC and PEC-based bactericidal techniques in the presence of halides to for inactivation of replication-deficient recombinant adenovirus (RDRADS). The specific study scope was to systematically evaluate and quantitatively compare the virucidal performance of PC and PEC treatment of RDRADS in the presence and absence of halides such as Cl^- and Br^-, using RDRADS encoding green fluorescent protein (GFP). The infectivity of the RDRADS can be accurately and conveniently determined using this method, because the virus encodes a GFP gene that can be expressed in host cells [28].

2. Materials and methods

2.1. Materials

Materials used for this study included indium tin oxide conducting glass slides (ITO, 8 Ω/square) from Delta Technologies Ltd. (USA), Titanium butoxide (97%), and other chemicals of analytical grade from Aldrich (unless otherwise stated). All solutions were prepared using high purity deionized water (Millipore Corp., 18 MΩ cm).

2.2. UV-LED array photoelectrochemical cell

All photocatalytic and photoelectrocatalytic disinfection experiments were performed in a UV-LED array thin layer electrochemical cell with a quartz window for illumination. The preparation of TiO_2 electrodes, cell configuration, and system set up were reported in detail, in our previous studies [26]. Briefly, the thickness of the reaction chamber and the illumination window area were 0.25 mm and 462 mm^2, respectively. A UV-LED array consisting of 4 pieces of UV-LED (NCCU033 (T), Nichia Corporation) was used as the light source. The emission electrum of the LED was centered at 365 nm with a spectrum half width of 8 nm. The UV intensity was adjusted by a power supply and measured with an UV-irradiance meter (UV-A, Beijing Normal University). A 0.1 M $NaNO_3$ was used as the supporting electrolyte. UV light intensity on the electrode surface was measured with an UV-irradiance meter (UV-A, Instruments of Beijing Normal University).

2.3. Viral strains, culture conditions and virus preparation

In this study, we used RDRADS encoding GFP as a model virus based on its sensitivity, specificity, and experimental safety. All experiments were performed in a biosafety level II laboratory and were conducted under appropriate conditions according to the Ref. [29]. A seed stock solution of the virus was obtained from the Experimental Medical Research Centre of Guangzhou Medical College. The viruses are replication deficient and can be propagated only in their packing cells. This feature enabled us to assay infected cells accurately, by counting cells with green fluorescence under a fluorescence microscope. The virus-containing cell was obtained by culturing with HEK293 (human embryonic kidney) cells and subsequent triple freezing of the infected cell culture in Dulbecco's-modified Eagle medium (DMEM) maintenance medium.

The viral suspension was purified using Sartobind Q 75 (Sartorius, Göttingen, Germany), according to the manufacturer menu. Prior to treatment, cell debris were removed by centrifugation at 3500 rpm for 15 min; the resulting supernatant was passed through a polyvinylidene fluoride (PVDF) MF membrane with nominal pore size of 0.22 μm. Then, 12.5 U/ml of nucleases (Takara Biotechnology (Dalian) Co., Ltd., China) were used to cleave the phosphodiester bonds between the nucleotide subunits of nucleic acids. The resulting viral suspension was passed through a centrifugal concentrator (100 000 MWCO) (Sartorius, Göttingen, Germany) to remove the salt. The virus concentrated with the centrifuge was finally diluted with sterilized H_2O to a desired concentration for the experiment. The initial population of RDRADS for each disinfection experiment was approximately 1000 Tissue Culture Infective Dose 50 (TCID50).

2.4. Inactivation of viruses and virological analytical procedure

Both PC and PEC disinfection experiments were performed under identical UV intensity using the same UV-LED array photoelectrochemical cell. For the PEC degradation experiments, a 0.1 M $NaNO_3$ solution was used as the supporting electrolyte, and a voltammograph (cv-27, BAS) was used for electrochemical control. Potential and current signals were monitored using a Macintosh computer (7220/200) coupled with a Maclab 400 interface (AD Instruments). A suspended solution containing a known number of RDRADS and 0.1 M of $NaNO_3$ prepared in sterilized tubes on a super clean bench was continuously injected into the cell via a precision pump during the inactivation process. The inactivation time of each sample was controlled by adjusting the flow rate. A sufficient volume of the inactivation sample was collected for further analysis after the system reached its steady-state. A 0.1 M $NaNO_3$ solution was used to clean the cell between the two sample injections. The samples collected after PEC treatment were analyzed the infectivity by green fluorescence of PK15 (pig kidney) cells. For assaying virus infectivity, 100 μl samples were added into 80% confluent PK15 cell monolayer (Fig. S1) in 48-well plates.

All of the disinfection experiments were repeated three times. The plates were rocked every 10–15 min during a 90 min cultured

period. Then, the inocula were replaced with DMEM containing 2% inactivated fetal bovine serum (Hyclone, SH), 100 U penicillin ml^{-1}, and 100 μg streptomycin ml^{-1}. The cells were then incubated at 37 °C for 48 h in a humidified incubator with a 5% CO_2 atmosphere. Because the number of viruses that infected each PK15 cell is variable, it is difficult to quickly quantify the PC and PEC removal efficiencies by counting the number of live viruses. However, the virus infectivity can be quantified by counting PK15 cells with green fluorescence, which is proportional to the virus numbers.

For PEC-Br/PEC-Cl disinfection experiments, the test solution with an additional 1.0 mM NaBr/NaCl was employed. The PC disinfection experiment was conducted under identical experimental conditions as the PEC experiment, except the electrochemical system was disconnected.

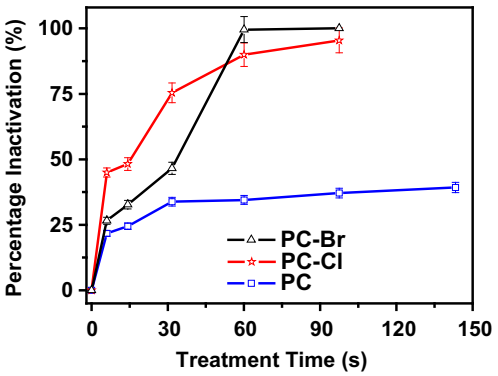

Fig. 2. PC inactivation efficiencies for RDRADS at nanoparticulate TiO_2 film photoanode in absence of halide ions (PC), in presence of 1.0 mM NaCl (PC-Cl), and 1.0 mM NaBr (PC-Br). The initial RDRADS population was ~1000 TCID50.

3. Results and discussion

First, the PC inactivation of RDRADS in the absence and presence of halides was carried out. The number of survived RDRADS was quantified from the fluorescence images (Fig. 1), using the method described in Ref. [28]. Fig. 2 shows the inactivation efficiency of PC treatment in the presence and absence of halide for samples containing an initial RDRADS about 1000 Tissue Culture Infective Dose 50 (TCID50). An initial rapid inactivation was observed for the PC treatment in the absence of halide. It took only 6.0 and 31.7 s to achieve 21.71 ± 1.1% and 33.82 ± 1.7% inactivation, respectively. However, dramatically reduced inactivation efficiencies were observed when the treatment time exceeded 30 s. It took another 111 s to achieve an additional 5.36% inactivation (i.e., 39.28 ± 2.0% at 143.2 s), suggesting PC treatment in the absence of halide cannot completely inactivate RDRADS within the treatment time investigated. Higher inactivation efficiencies may be achievable if a longer treatment time is employed.

As demonstrated in our previous study, adding halide ions such as Br^- can dramatically enhance the photocatalytic inactivation efficiency for bacteria [26]. As such, similar approaches were adopted in this work to inactivate RDRADS. Fig. 2 also shows the inactivation performance of PC treatment in presence of 1.0 mM Cl^- (PC-Cl). These results show that the inactivation percentages rapidly increased during the first 10 s of PC-Cl treatment. A 44.97 ± 1.7% inactivation was achieved within 6.0 s, compared to a 21.71 ± 1.1% inactivation achieved by PC treatment over the same period without Cl^-. Such an inactivation percentage achieved by PC-Cl treatment was even higher than that of a 143.2 s PC treatment in the absence of Cl^- (39.28 ± 2.0%). When further increasing the treatment time, PC-Cl inactivation percentages steadily increased to 75.39 ± 3.8% at 31.7 s, and 95.43 ± 4.8% at 97.5 s.

The inactivation performance of PC treatment in presence of 1.0 mM Br^- (PC-Br) for RDRADS is also shown in Fig. 2. The inactivation percent increased with the treatment time, achieving 26.56 ± 1.3%, 32.73 ± 1.6%, and 46.59 ± 2.3% inactivation at 6.0, 14.3, and 31.7 s, respectively. When compared to PC-Cl treatment, PC-Br revealed a relatively slow inactivation during the initial 30 s treatment period. These achieved inactivation percentages are just slightly higher than those of PC treatment in absence of halide (i.e., 21.71 ± 1.1%, 24.48 ± 1.2%, and 33.82 ± 1.7% at 6.0, 14.3, and 31.7 s,

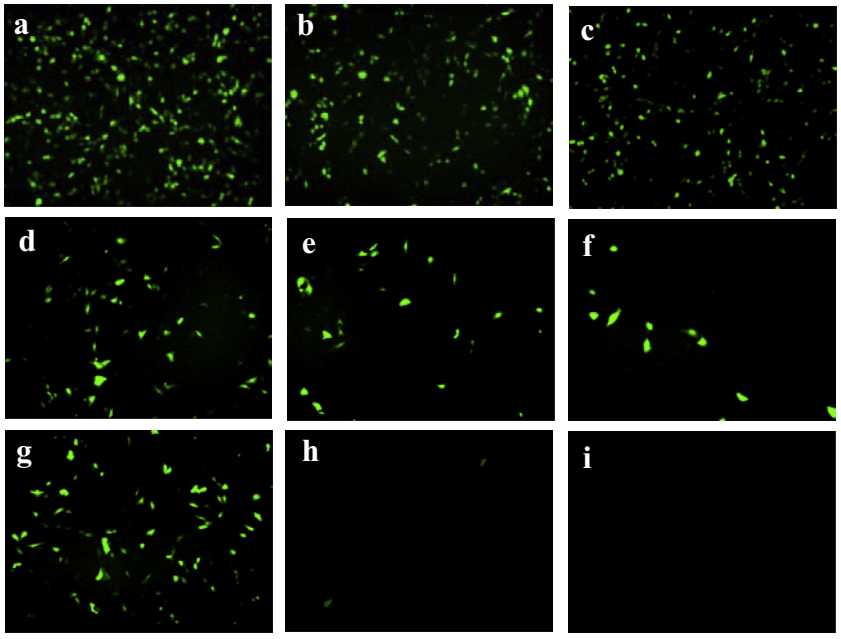

Fig. 1. Representative micrograph (magnification: 100×) PK15 cells infected with GFP expressed virus under different photocatalytic inactivation treatment times in the absence of halide ions [(a) 0 s, (b) 31.7 s, and (c) 143.2 s], in the presence of NaCl [(d) 31.7 s, (e) 60.1 s, and (f) 97.5 s] or NaBr [(g) 3.17 s, (h) 60.1 s, and (i) 97.5 s].

respectively), but significantly lower than those of PC-Cl treatment (i.e., 44.97 ± 1.7%, 48.23 ± 2.4%, and 75.39 ± 3.8% at 6.0, 14.3, and 31.7 s, respectively). However, the inactivation performance of PC-Br treatment outperformed PC-Cl treatment with extended treatment time (e.g., >60 s), inactivating 99.55 ± 5.0% and 100% of RDRADS within 60.1 and 97.5 s, respectively.

In addition, we compared the effect of the type of halides on the inactivation performances under PC treatment. The inactivation ratios obtained from PC-Br and PC-Cl treatments were found to be between 0.60 and 0.68 within 30 s, respectively, suggesting that the presence of Cl^- (PC-Cl) is more effective than that of Br^- (PC-Br) with PC treatments during the initial 30 s.

The high efficiency of PEC has been widely acknowledged [24,30]. The applied potential bias to timely remove the photogenerated electrons and physically separate the photoanode from the cathode are generally regarded as the main factors leading to the enhanced photocatalytic efficiency [31,32]. It has also been recognized that the applied potential bias prolongs the lifetime of photoholes, enabling direct photohole reactions [30]. Despite numerous studies on PEC degradation of organics have been previously reported [24,30,32], based on the literature, it appears that the PEC inactivation of viruses has been rarely attempted [25]. Therefore, PEC inactivation of RDRADS was also investigated in the absence and presence of halides.

Fig. 3 shows the representative micrograph of PK15 cells infected with GFP expressed virus under different photoelectrocatalytic inactivation treatment times at a nanoparticulate TiO_2 photoanode in a continuous flow-though cell in the absence of halide ions. Fig. 4 shows the PEC inactivation performance for RDRADS in the presence and absence of halides. Without adding halides, a 43.50 ± 2.2% inactivation percentage can be achieved at 9.8 s, indicating a drastically enhanced performance within shorter treatment period (e.g., <10 s) when compared to PC treatment in the absence of halide. However, the inactivation dramatically slowed down and then leveled off at ca. 45% when the treatment time was further increased beyond 15 s. Fig. 4 also shows PEC inactivation performance for RDRADS in the presence of 1.0 mM Cl^- (PEC-Cl). It was found that a 49.83 ± 2.5% inactivation can be achieved within 6.0 s of PEC-Cl treatment. The inactivation percentage increased almost linearly from 49.83 ± 2.5% to 88.10 ± 4.4% within the treatment period between 6.0 and 31.7 s.

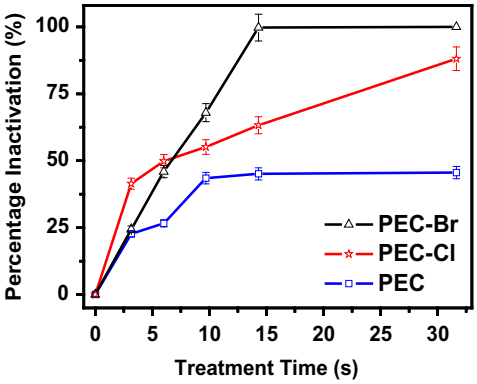

Fig. 4. PEC inactivation efficiencies for RDRADS at nanoparticulate TiO_2 film photoanode in absence of halide ions (PEC), in present of 1.0 mM NaCl (PEC-Cl), and 1.0 mM NaBr (PEC-Br). The initial populations of RDRADS were ~1000 TCID50.

Fig. 4 also shows the inactivation performance of PEC in the presence of 1.0 mM Br^- (PEC-Br). The inactivation percentages increased almost linearly with the treatment time up to 14.3 s, achieving a 99.77 ± 5.0% inactivation. A 100% inactivation was achieved at 31.7 s. Such an inactivation performance is the highest among all methods investigated in this work, demonstrating the superiority of PEC-Br treatment. The results also show that the inactivation percentages of PEC-Br treatment within a short treatment period (i.e., 0 ~ 6.0 s) was lower than that of PEC-Cl treatment, but surpassed the PEC-Cl treatment when the treatment time was greater than 9.8 s.

In addition, we also compared the effect of halide type on inactivation performances under PEC treatment. The inactivation ratios obtained in the presence of Br^- (PEC-Br) and Cl^- (PEC-Cl) were found to be below 1 (0.92) during the initial 6.0 s, suggesting a better initial inactivation ability of the PEC-Cl treatment. The PEC-Br's performance surpassed the PEC-Cl treatment with extended treatment time as demonstrated by the ratios of 1.58 and 1.14 obtained after 14.3 and 31.7 s treatments, respectively.

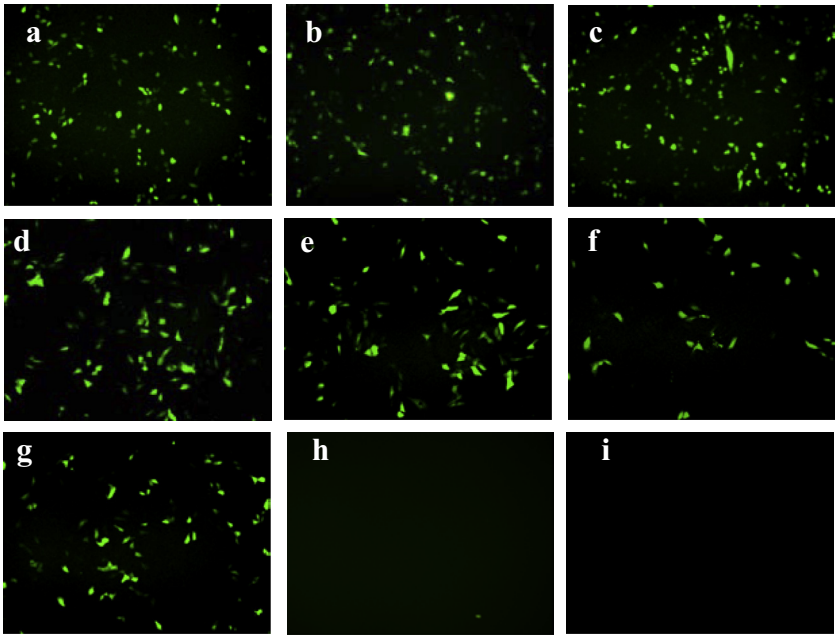

Fig. 3. Representative micrograph (magnification: 100×) PK15 cells infected with GFP expressed virus under different photoelectrocatalytic inactivation treatment times at a nanoparticulate TiO_2 photoanode in a continuous flow-though cell in absence of halide ions [(a) 9.8 s, (b) 14.3 s, and (c) 31.7 s], in the presence of NaCl [(d) 9.8 s, (e) 14.3 s, and (f) 31.7 s] or NaBr [(g) 9.8 s, (h) 14.3 s, and (i) 31.7 s].

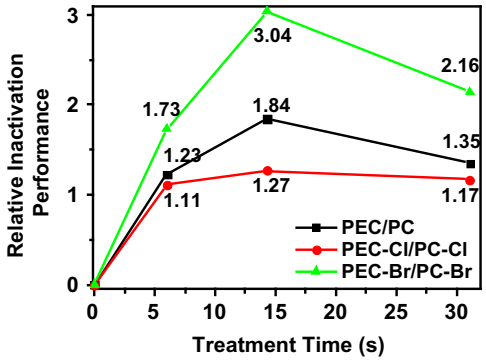

Fig. 5. Relative inactivation performance of different treatments.

Fig. 5 summarizes the relative inactivation performances of different treatments investigated in this study. Considering that all experiments were performed using the same photoelectrochemical cell, under the same light intensity and using the same initial virus concentration, the comparison data shown in Fig. 5 are of quantitative and truly reflect the virus inactivation abilities of different treatments. The ratios of PEC to PC treatments in the presence and absence of halides were greater than 1 for all cases investigated, confirming that PEC treatments are more effective than that of PC treatments under comparable conditions. It can be seen that comparing to PC, PC-Cl, and PC-Br treatments, the corresponding PEC treatments are 1.23–1.84, 1.11–1.27 and 1.73–3.04 times more effective, respectively.

These experimental results confirm that the photocatalytic inactivation efficiency can be enhanced in presence of low concentration halides (X^-) and further enhanced by applying potential bias onto the anode in PEC system. It is commonly agreed that for a TiO_2 photocatalysis-based method, the photocatalytically generated active oxygen species (AOSs) are responsible for inactivation [33,34]. The enhanced inactivation performance for PC-X treatments is due to the production of additional viricides, resulting from the photocatalytic oxidation of X^- (see Eq. (1)) [35,36].

$$TiO_2\{h^+_{VB}\} \xrightarrow{X^-} \{X^{\cdot}/X^{\cdot-}_2, X_2, HOX/OX^-\} \quad (1)$$

The further enhanced inactivation performance for PEC-X treatments can be attributed to the increased productions of AOSs and X-based viricides, and prolonged lifetime of photoholes (h^+) for direct inactivation [30]. Fig. 6 shows the photocurrent responses obtained from 0.1 M $NaNO_3$ solution and 0.1 M $NaNO_3$ solution containing Br^- or Cl^- at a given concentration. In the absence of X^-, the photocurrent is originated from the photocatalytic oxidation of water, which is directly proportional to the production rate of AOSs [24,32]. An increase in halide ions concentration leads to an increase in the photocurrent. The net photocurrent increase results from the photocatalytic oxidation of halides, which should be directly proportional to the production rate of X-based viricides (e.g., $X^{\cdot}/X^{\cdot-}_2$, X_2, HOX/XO^-) [26].

The photocatalytic inactivation process at TiO_2 is an essential oxidation process. The roles of AOSs and h^+ have been widely reported [33,34]. However, which of the X-based viricides (e.g., $X^{\cdot}/X^{\cdot-}_2$, X_2, HOX/XO^-) generated from photocatalytic oxidation of X^- need to be further discussed. Considering the relatively low standard potentials of Cl_2/Cl^- and Br_2/Br^- (+1.36 and +1.087 V, respectively), it is unlikely that these halogen species are the main contributors to the enhancement inactivation efficiency. Moreover, the standard potentials of $HOCl/Cl^-$ and $HOBr/Br^-$ are +1.63 and +1.33 V, respectively. Although the oxidation power of these species are not high, they should be sufficient to cause damage to the capsid of nonenveloped viruses (such as adenovirus), whose capsid is composed of protein polypeptides. Also, HOX prefers to react with amino acids with an amino group side chains [38], and is particular effective to inactivate proteins containing sulfhydryl groups [38]. Therefore, HOX could play an important role in the damage of the protein capsid of RDRADS.

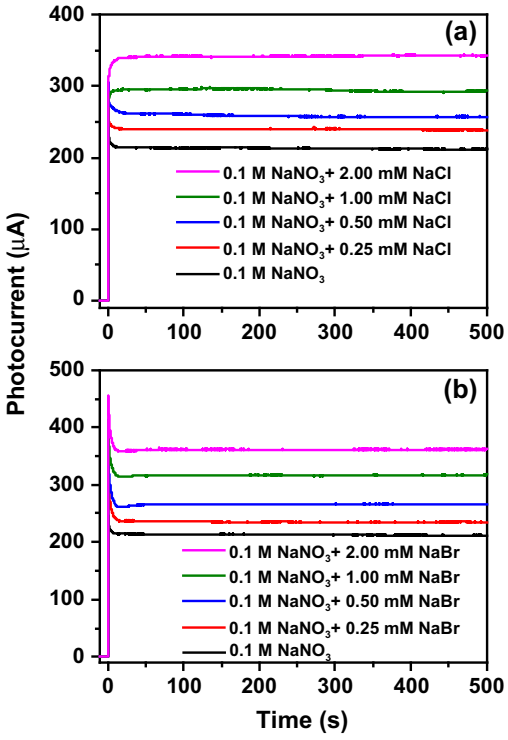

Fig. 6. Photocurrent–time profiles obtained from solutions containing 0.1 M $NaNO_3$ and different concentrations of (a) NaCl and (b) NaBr under a typical light intensity of 8.0 mW/cm^2 (measured at 365 nm) and applied potential bias of +0.30 V vs Ag/AgCl.

The photocatalytically generated $X^{\cdot}$ should be considered a dominant contributor to the enhanced virucidal efficiency due to its reactive nature, strong oxidation power ($E^0[Cl^{\cdot}/Cl^-]$ = +2.41 V [39] and $E^0[Br^{\cdot}/Br^-]$ = +1.96 V [40]), and its ability to form stable di-halide radical anions ($X^{\cdot-}_2$) [41]. The formation of $X^{\cdot-}_2$ prolongs the lifetime of $X^{\cdot}$ to maximize the inactivation effect. These oxidative radicals could rapidly damage the protein capsid and invade viruses to further damage the intracellular macromolecules (such as nucleic acids). It should be noted that X^- serves as an electron mediator during the photocatalytic inactivation process [26]. It is photocatalytically oxidized at the illuminated TiO_2 surface to form the reactive species and regenerated when reacting with virus (see Eq. (2)). This is the prime reason that only a very low concentration of X^- is required to achieve the purpose.

$$TiO_2\{h^+_{VB}\} + Br^- \rightarrow Br^{\cdot}/Br^{\cdot-}_2 \xrightarrow{Virus} Br^- + \text{Damaged virus} \quad (2)$$

However, it worth mentioning that compared to the PEC-Cl treatment, higher inactivation efficiency of the PEC-Br treatment could be attributed to the higher concentration of $Br^{\cdot-}_2$ in the PEC-Br system. This is because the reaction equilibrium constant for the formation of $Br^{\cdot-}_2$ ($K = 3.9 \times 10^5\ M^{-1}$) is higher than that of $Cl^{\cdot-}_2$ ($K = 1.4 \times 10^5\ M^{-1}$) in the PEC-Cl system [42].

In comparison to our previous work [26], the RDRADS is more difficult to be photocatalytically inactivated than bacteria. A possible reason could be that RDRADS is a double-stranded DNA virus, so the damaged DNA could be rapidly repaired by a host cell enzymes [43]. Also, unlike the complex cell wall and inner membrane structures of bacteria, viruses lack enzymes and other sensitive systems, enabling the virus to prolong its survival outside the body environment [44].

4. Conclusions

In summary, the virucidal performance of PC and PEC treatments in the presence and absence of halides are investigated and meaningfully compared under comparable experimental conditions. The results confirm that the virucidal efficiency can be enhanced in presence of a low concentration of halides and further enhanced by applying photoelectrocatalysis. The PEC-Br treatment shows the best virucidal performance, capable of completely inactivating a ~1000 TCID50 RDRADS population within 31.7 s. The superior virucidal performances of PEC-X treatments can be attributed to the increased production of AOSs and X-based viricides, and prolonged lifetime of h^+ for direct inactivation. The findings of this work confirm that new forms of active species generated in situ via a PC or PEC process are effective for not only bacteria, but also viruses. In theory, the proposed method can be used to kill other types of viruses and to decompose organic pollutants.

Acknowledgments

This is contribution No. IS–1893 from GIGCAS. This work was supported by Australian Research Council and NSFC (No. 21077104), Knowledge Innovation Program of Guangzhou Institute of Geochemistry, CAS (GIGCX-10-01) and General Research Fund (GRF 476811) to P.K. Wong.

Appendix A. Supplementary data

Supplementary data associated with this article can be found, in the online version, at http://dx.doi.org/10.1016/j.cej.2014.05.059.

References

[1] WHO, Cumulative number of reported probable cases of severe acute respiratory syndrome (SARS). in, 2003.
[2] H. Heinonen-Tanski, T. Reponen, J. Koivunen, Airborne enteric coliphages and bacteria in sewage treatment plants, Water Res. 43 (2009) 2558–2566.
[3] M.V. Liga, E.L. Bryant, V.L. Colvin, Q. Li, Virus inactivation by silver doped titanium dioxide nanoparticles for drinking water treatment, Water Res. 45 (2011) 535–544.
[4] F. Bosshard, F. Armand, R. Hamelin, T. Kohn, Mechanisms of human adenovirus inactivation by sunlight and uvc light as examined by quantitative PCR and quantitative proteomics, Appl. Environ. Microbiol. 79 (2013) 1325–1332.
[5] A. Matin, Z. Khan, S.M.J. Zaidi, M.C. Boyce, Biofouling in reverse osmosis membranes for seawater desalination: phenomena and prevention, Desalination 281 (2011) 1–16.
[6] A.C. Eischeid, J.A. Thurston, K.G. Linden, UV disinfection of adenovirus: present state of the research and future directions, Crit. Rev. Environ. Sci. Technol. 41 (2011) 1375–1396.
[7] G.A. Shin, M.D. Sobsey, Inactivation of norovirus by chlorine disinfection of water, Water Res. 42 (2008) 4562–4568.
[8] D. Liviac, E.D. Wagner, W.A. Mitch, M.J. Altonji, M.J. Plewa, Genotoxicity of water concentrates from recreational pools after various disinfection methods, Environ. Sci. Technol. 44 (2010) 3527–3532.
[9] Y. Wang, Q. Wang, B.Y. Gao, Q.Y. Yue, Y.X. Zhao, The disinfection by-products precursors removal efficiency and the subsequent effects on chlorine decay for humic acid synthetic water treated by coagulation process and coagulation–ultrafiltration process, Chem. Eng. J. 193 (2012) 59–67.
[10] J.L. Acero, F.J. Benitez, F.J. Real, G. Roldan, E. Rodriguez, Chlorination and bromination kinetics of emerging contaminants in aqueous systems, Chem. Eng. J. 219 (2013) 43–50.
[11] M.Y. Lim, J.M. Kim, J.E. Lee, G. Ko, Characterization of ozone disinfection of murine norovirus, Appl. Environ. Microbiol. 76 (2010) 1120–1124.
[12] AWWA, Water Treatment: Principles and Practices of Water Supply Operations, American Water Works Association, Denver, 1995.
[13] K.E. O'Shea, D.D. Dionysiou, Advanced oxidation processes for water treatment, J. Phys. Chem. Lett. 3 (2012) 2112–2113.
[14] D. Gerrity, H. Ryu, J. Crittenden, M. Abbaszadegan, Photocatalytic inactivation of viruses using titanium dioxide nanoparticles and low-pressure UV light, J. Environ. Sci. Health A 43 (2008) 1261–1270.
[15] H. Ishiguro, Y. Yao, R. Nakano, M. Hara, K. Sunada, K. Hashimoto, J. Kajioka, A. Fujishima, Y. Kubota, Photocatalytic activity of Cu^{2+}/TiO_2-coated cordierite foam inactivates bacteriophages and *Legionella pneumophila*, Appl. Catal. B Environ. 129 (2013) 56–61.
[16] H.R. Jafry, M.V. Liga, Q.L. Li, A.R. Barron, Simple route to enhanced photocatalytic activity of P25 titanium dioxide nanoparticles by silica addition, Environ. Sci. Technol. 45 (2011) 1563–1568.
[17] USEPA, The drinking water candidate contaminant list, (2005).
[18] Z. Barna, M. Kadar, The risk of contracting infectious diseases in public swimming pools. A review, Ann. I. Super. Sanita. 48 (2012) 374–386.
[19] S.C. Jiang, Human adenoviruses in water: occurrence and health implications: a critical review, Environ. Sci. Technol. 40 (2006) 7132–7140.
[20] H.D. Silva, M.T.A. Garcia-Zapata, C.E. Anunciacao, Why the use of adenoviruses as water quality virologic marker?, Food Environ Virol. 3 (2011) 138–140.
[21] N.A. Ballester, J.P. Malley, Sequential disinfection of adenovirus type 2 with UV-chlorine–chloramine, J. Am. Water Works Ass. 96 (2004) 97–103.
[22] G. La Rosa, M. Fratini, S. della Libera, M. Iaconelli, M. Muscillo, Emerging and potentially emerging viruses in water environments, Ann. I. Super. Sanita. 48 (2012) 397–406.
[23] J. Van Heerden, M.M. Ehlers, W.B. Van Zyl, W.O.K. Grabow, Incidence of adenoviruses in raw and treated water, Water Res. 37 (2003) 3704–3708.
[24] H.J. Zhao, D.L. Jiang, S.Q. Zhang, W. Wen, Photoelectrocatalytic oxidation of organic compounds at nanoporous TiO_2 electrodes in a thin-layer photoelectrochemical cell, J. Catal. 250 (2007) 102–109.
[25] M. Cho, E.L. Cates, J. Kim, Inactivation and surface interactions of MS-2 bacteriophage in a TiO_2 photoelectrocatalytic reactor, Water Res. 45 (2011) 2104–2110.
[26] G.Y. Li, X.L. Liu, H.M. Zhang, T.C. An, S.Q. Zhang, A.R. Carroll, H.J. Zhao, In situ photoelectrocatalytic generation of bactericide for instant inactivation and rapid decomposition of gram-negative bacteria, J. Catal. 277 (2011) 88–94.
[27] G.Y. Li, X.L. Liu, H.M. Zhang, P.K. Wong, T.C. An, H.J. Zhao, Comparative studies of photocatalytic and photoelectrocatalytic inactivation of *E. coli* in presence of halides, Appl. Catal. B Environ. 140–141 (2013) 225–232.
[28] X.Y. Li, Q.C. Liu, X.H. Bi, G.Y. Sheng, J.M. Fu, P.X. Ran, B. Li, An in vitro model to evaluate virus aerosol characteristics using a GFP-expressing adenovirus, J. Med. Microbiol. 57 (2008) 1335–1339.
[29] T.C. He, S.B. Zhou, L.T. da Costa, J. Yu, K.W. Kinzler, B. Vogelstein, A simplified system for generating recombinant adenoviruses, Proc. Natl. Acad. Sci. U.S.A. 95 (1998) 2509–2514.
[30] D.L. Jiang, S.Q. Zhang, H.J. Zhao, Photocatalytic degradation characteristics of different organic compounds at TiO_2 nanoporous film electrodes with mixed anatase/rutile phases, Environ. Sci. Technol. 41 (2007) 303–308.
[31] P.A. Mandelbaum, A.E. Regazzoni, M.A. Blesa, S.A. Bilmes, Photo-electro-oxidation of alcohols on titanium dioxide thin film electrodes, J. Phys. Chem. B 103 (1999) 5505–5511.
[32] H.J. Zhao, D.L. Jiang, S.Q. Zhang, K. Catterall, R. John, Development of a direct photoelectrochemical method for determination of chemical oxygen demand, Anal. Chem. 76 (2004) 155–160.
[33] H. Selcuk, H.Z. Sarikaya, M. Bekbolet, M.A. Anderson, Bromate formation on the non-porous TiO_2 photoanode in the photoelectrocatalytic system, Chemosphere 62 (2006) 715–721.
[34] T. Bak, J. Nowotny, N.J. Sucher, E. Wachsman, Effect of crystal imperfections on reactivity and photoreactivity of TiO_2 (rutile) with oxygen, water, and bacteria, J. Phys. Chem. C 115 (2011) 15711–15738.
[35] L.A.T. Espinoza, F.H. Frimmel, Formation of brominated products in irradiated titanium dioxide suspension containing bromide and dissolved organic carnon, Water Res. 42 (2008) 1778–1784.
[36] H. Noguchi, A. Nakajima, T. Watanabe, K. Hashimoto, Design of a photocatalyst for bromate decomposition: Surface modification of TiO_2 by pseudo-boehmite, Environ. Sci. Technol. 37 (2003) 153–157.
[37] G.R. Dychdala, Chlorine and chlorine compounds, in: Disinfection, Sterilization and Preservation, fourth ed., Lea & Febiger, Philadelphia, PA, USA, 1991, pp. 131–151.
[38] W.E. Knox, P.K. Stumpf, D.E. Green, V.H. Auerbach, The inhibition of sulfhydryl enzymes as the basis of the bactericidal action of chlorine, J. Bacteriol. 55 (1948) 451–458.
[39] J.E. Rogers, B. Abraham, A. Rostkowski, L.A. Kelly, Mechanisms of photoinitiated cleavage of DNA by 1,8-naphthalimide derivatives, Photochem. Photobiol. 74 (2001) 521–531.
[40] G. Merenyi, J. Lind, Reaction-mechanism of hydrogen abstraction by the bromine atom in water, J. Am. Chem. Soc. 116 (1994) 7872–7876.
[41] M.M. Cheng, A. Bakac, Photochemical oxidation of halide ions by a nitratochromium(III) complex. Kinetics, mechanism, and intermediates, J. Am. Chem. Soc. 130 (2008) 5600–5605.
[42] Y. Liu, A.S. Pimentel, Y. Antoku, B.J. Giles, J.R. Barker, Temperature-dependent rate and equilibrium constants for $Br^{\cdot}(aq) + Br^{-}(aq) \leftrightarrow Br_2^{-\cdot}(aq)$, J. Phys. Chem. A 106 (2002) 11075–11082.
[43] C.P. Gerba, D.M. Gramos, N. Nwachuku, Comparative inactivation of enteroviruses and adenovirus 2 by UV light, Appl. Environ. Microbiol. 68 (2002) 5167–5169.
[44] J.M. Montgomery, Water Treatment Principles and Design, John Wiley & Sons, New York, N.Y., 1985. 262–283.